# IMPACT OF INCORPORATING GRAPHENE NANOPLATELET DISPERSIONS ON STRENGTH DEVELOPMENT OF LOW-CARBON CEMENTITIOUS MATRICES

**Ernests Ozolins[1], Arturs Macanovskis[2], Nikola Sinica[2], Maris Tupesis[2]**
[1]SIA "Dzelzsbetons MB", Latvia; [2]SIA "Betona petijumu centrs", Latvia
ernests.ozolins@mbbetons.lv, arturs.macanovskis@bpcentrs.lv,
nikola.sinica@bpcentrs.lv, maris.tupesis@bpcentrs.lv

**Abstract.** The precast concrete industry faces the dual challenge of decarbonisation and the requirement for rapid early-age strength development. While CEM III binders significantly reduce global warming potential, they suffer from slow hydration kinetics, typically delivering insufficient 24-hour demoulding strength. This research investigates the curing-accelerating potential of graphene nanoplatelet (GNP) dispersions acting as heterogeneous nucleation seeds in cementitious matrices with varying slag content. Experimental mortar samples were produced according to EN 196-1 across two test series. In the conventional dosage series, three binder systems (CEM I 52.5N, CEM III/B 32.5N, CEM II/B-M 52.5N) were investigated at pure graphene dosages of 0.02-0.10% by binder mass at w/c 0.50; hardened specimen density was determined according to EN 12390-7. In the microdosing series, pure graphene contents of 0.0002-0.0014% by binder mass were applied to CEM II/B-M, CEM III/B, and a hybrid CEM III/B + CEM I blend. Compressive strength was assessed at 24 hours, 7 days, and 28 days and flexural strength at 7 and 28 days. Results indicate a strongly binder-dependent and dosage-dependent response. In the conventional series, slag-containing systems showed strength reductions and systematic density decreases consistent with surfactant-induced air entrainment, whilst CEM I exhibited slight densification, consistent with a binder-chemistry-driven mechanism while still reducing strength. In the microdosing series, CEM II/B-M was the only system to show consistent indicative positive strength gains, reaching 5% at 24 hours, with gains persisting to 28 days. CEM III/B and the hybrid blend showed reductions at all ages. These findings indicate that binder chemistry governs the graphene dispersion effect even at concentrations far below those previously reported, and that beneficial effects in compatible systems appear to persist to 28 days; confirmation through replicated testing is recommended.

**Keywords:** graphene nanoplatelets (GNPs), low-carbon concrete, concrete strength development, heterogeneous nucleation.

## Introduction

The construction sector's transition toward sustainable, low-carbon manufacturing presents one of the most significant industrial challenges, with Portland cement production alone accounting for an estimated 6-10% of global $CO_2$ emissions [1-3]. Reducing the carbon footprint of concrete has driven widespread adoption of supplementary cementitious materials (SCMs), particularly ground granulated blast-furnace slag (GGBS), a by-product of iron production with latent hydraulic properties that can replace a significant proportion of Portland cement clinker [4; 5]. High-slag binders such as CEM III, can substantially reduce the embodied carbon of the binder fraction while achieving long-term strengths comparable to ordinary Portland cement. However, the slow hydration kinetics of slag result in significantly lower early-age strength development, which results in a critical challenge for the precast concrete industry, where achieving sufficient compressive strength within 24 hours or less is an operational necessity for demoulding and maintaining production cycle times [6].

High-slag cements, designated as CEM III contain GGBS as significant proportion of binder by mass, offering substantial reductions in embodied carbon footprint compared to ordinary Portland cement (CEM I). The latent hydraulic properties of slag enable long-term strength development through the formation of additional calcium silicate hydrate (C-S-H) phases, often resulting in ultimate strengths comparable to or exceeding those of Portland cement systems long term [7]. However, this advantage comes with a significant practical limitation, the slow hydration kinetics of slag result in considerably lower early-age strengths, particularly within the first 72 hours [6]. In precast concrete production, production cycle times depend on achieving a minimum demoulding strength, and the delayed strength development of slag-rich binders can substantially increase operational costs and reduce production throughput.

Recent advances in nanotechnology have enabled alteration of cement hydration kinetics and matrix microstructure. Graphene nanoplatelets (GNPs), consisting of few-layer stacks of graphene with lateral dimensions in the micrometre range and thicknesses of a few nanometres, have emerged as a promising class of nanomaterial additives for cementitious systems [8; 9]. Their exceptional specific surface area

(typically 300-750 $m^2 \cdot g^{-1}$), two-dimensional morphology, and surface chemistry have been proposed to enable multiple reinforcement mechanisms such as heterogeneous nucleation seeding that accelerates hydration, nano-filler effects that densify the cement paste matrix, and micro-crack bridging that enhances fracture resistance [10-12].

The literature on graphene-based reinforcement of cementitious materials spans a wide range of graphene derivatives and dosages. Studies using graphene oxide (GO), a chemically oxidised, hydrophilic derivative, have reported compressive strength improvements of 15-90% at dosages typically between 0.03% and 0.10% by weight of binder [13; 14]. For pristine graphene and few-layer graphene (FLG), the reported effective dosage range is comparable, optimum performance is most commonly observed between 0.05% and 0.15% by weight of cement, with the majority of published studies not investigating dosages below 0.05% [15; 16]. The pure graphene contents applied in the present microdosing series (0.0002-0.0014% by binder mass) therefore fall 7 to 70 fold below the lowest FLG dosage documented in the published literature, representing a previously unexplored concentration regime. Very recently, a small number of studies have begun to probe ultra-low dosages of GO in cement systems, identifying meaningful microstructural and durability effects at concentrations as low as 0.001-0.006% by binder weight. For FLG, however, no published study has systematically investigated dosages below 0.01%, representing a notable gap in the fundamental understanding of graphene–cement interaction at trace concentrations.

Irrespective of graphene type and dosage, a recurring challenge is the effective dispersion of hydrophobic graphene particles within the aqueous cement system. Due to high surface energy and strong inter-platelet van der Waals forces, GNPs tend to reaggregate rapidly in aqueous media, severely limiting their reinforcing potential [17; 18]. Commercially available surfactant-stabilised aqueous dispersions offer a practical and scalable solution; however, the presence of surfactants introduces additional chemical variables that may interact with cement hydration, particularly in complex multi-component binder systems [19]. A critical distinction that has received limited attention in the literature is that there is a significant difference in performance between the pure, dry graphene materials used in most academic studies and the commercial surfactant-stabilised dispersions that are relevant to industrial practice.

Despite the extensive body of research on graphene-based cement composites, the overwhelming majority of published studies employ ordinary Portland cement (CEM I) as the sole binder. High-slag blended systems, which are directly relevant to low-carbon precast construction and the concrete industry in general, have received very limited attention. Only a small number of investigations have examined carbon-based nanomaterials in GGBS containing binders, and these have focused primarily on hydration calorimetry rather than mechanical performance across multiple ages [20; 21]. Portland-limestone composite cements (CEM II/B-M type) appear to be entirely unstudied in this context.

This study addresses the gap in understanding how commercially available surfactant-stabilised GNP dispersions interact with different cement matrices, with emphasis on high-slag systems relevant to low-carbon precast construction. The objectives were to evaluate the early-age, 7-day, and 28-day strength response of different cement systems to GNP dispersion addition across a conventional and an ultra-low (microdosing) dosage regime, identify dosage-dependent trends in both strength and density, and assess the compatibility of commercial surfactant-stabilised dispersions with different cement chemistries.

## Materials and methods

Materials used in the study:

- CEM II B-M (S-LL) 52.5 N cement;
- CEM III/B 32.5N-LH $\cdot s^{-1}$R cement;
- CEM I 52.5 N cement;
- standard Sand 1350 g in each pack according to EN 196-1;
- tap water;
- graphene admixture (with mean particle size of 816 nm, particle distribution in Fig. 1, graphene concentration of 15.07 g/l, with PCE surfactant).

The graphene admixture was incorporated into standard cement mortar across two experimental series. In the conventional additive dosage series, total pure graphene dosages of 0.02-0.10%, by binder mass were applied to three binder systems (CEM I, CEM III/B, and CEM II/B-M) at w/c 0.50 and in 0.02% increments of graphene addition. In the microdosing series, three systems were investigated at pure graphene concentrations of 0.0002-0.0014% by binder mass: CEM II/B-M, CEM III/B, and a hybrid CEM III/B + CEM I 52.5N blend. A full list of mix proportions for the microdosing additive series is presented in Table 1.

Table 1

**Mortar mix proportions used in this study**

| Reference | CEM II, g | CEM III B, g | CEM I, g | Water to cement ratio | Pure graphene dosage, % of binder |
|---|---|---|---|---|---|
| S – 1 | - | 450 | - | 0.5 | 0.0000 |
| S – 2 | - | 450 | - | 0.5 | 0.0002 |
| S – 3 | - | 450 | - | 0.5 | 0.0005 |
| S – 4 | - | 450 | - | 0.5 | 0.0007 |
| S – 5 | - | 450 | - | 0.5 | 0.0011 |
| S – 6 | - | 450 | - | 0.5 | 0.0014 |
| S – 7 | 450 | - | - | 0.5 | 0.0000 |
| S – 8 | 450 | - | - | 0.5 | 0.0002 |
| S – 9 | 450 | - | - | 0.5 | 0.0005 |
| S – 10 | 450 | - | - | 0.5 | 0.0007 |
| S – 11 | 450 | - | - | 0.5 | 0.0011 |
| S – 12 | 450 | - | - | 0.5 | 0.0014 |
| S – 13 | - | 346.5 | 103.5 | 0.5 | 0.0000 |
| S – 14 | - | 346.5 | 103.5 | 0.5 | 0.0002 |
| S – 15 | - | 346.5 | 103.5 | 0.5 | 0.0005 |
| S – 16 | - | 346.5 | 103.5 | 0.5 | 0.0007 |
| S – 17 | - | 346.5 | 103.5 | 0.5 | 0.0011 |
| S – 18 | - | 346.5 | 103.5 | 0.5 | 0.0014 |

Compressive strength was assessed at 24 hours, 7 days, and 28 days on 40×40×40 mm cube specimens obtained by cutting 40×40×160 mm prisms, and flexural strength at 7 days and 28 days on the prisms, in accordance with EN 196-1. Testing was performed using a compression testing machine with a loading rate of 2400 $N \cdot s^{-1}$. Two specimens were tested at each age; results are reported as mean values with error bars indicating the range between the two measurements. This reduced replication was adopted in order to maximise the number of binder systems and dosage levels investigated within the constraints of a single experimental programme, and is consistent with the exploratory, screening-level intent of the study. With $n = 2$ specimens per condition, no standard deviation, coefficient of variation, or formal significance test can be meaningfully derived, error bars therefore represent the full range between the two measurements rather than a statistical confidence interval, and all reported differences should be interpreted as indicative trends rather than statistically verified effects. Hardened sample density was determined by the water immersion method in accordance with EN 12390-7, applied to the conventional additive dosage series only. Results are reported as percentage change relative to the GNP-free reference mix for each binder type.

For precise measurements, scales (LW Measurements HRB series) with an accuracy of 0.01 g were used for cement, whilst graphene admixture and water were weighed using scales (RADWAG PS 1000.R2) with a precision of 0.001 g. Cement paste was mixed using a standard mortar mixer according to EN 196-1 procedures, modified for GNP addition. The GNP dispersion was first combined with the mixing water and poured into the mixing bowl, then cement was added gradually over 30 seconds at low mixer set to low speed (140 rpm), then sand was added and the mix was further mixed for 30 seconds at low speed, followed by 30 seconds at high speed (285 rpm), 90-second rest period when the material stuck at the sides of the bowl was cleaned off, and the final 60 seconds at high speed. After casting, specimens were covered with polyethylene sheeting and maintained at 20 ± 2 °C and > 95% relative

humidity. Moulds were stripped after 24 hours for early-age testing or continued curing in water at 20 ± 2 °C until the designated test age. Error bars in figures represent the maximum and minimum obtained values across all similar specimens tested.

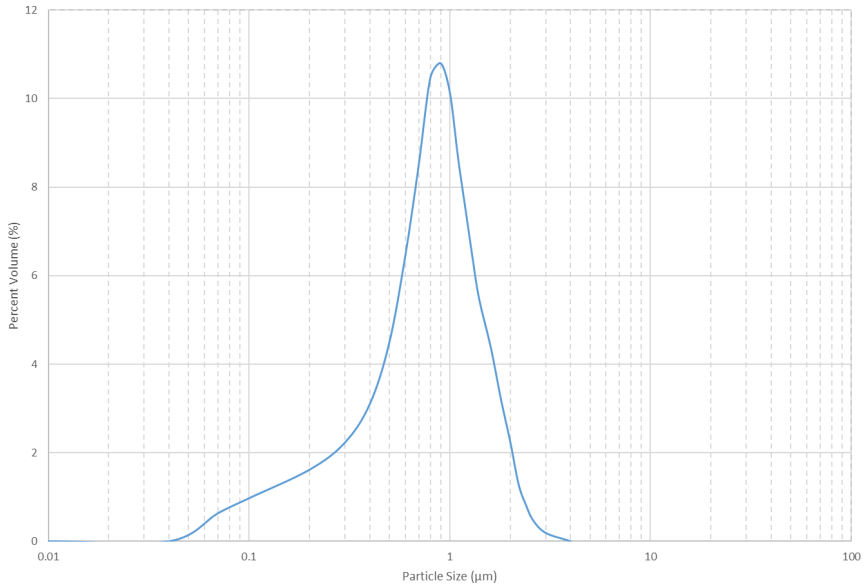


Fig. 1. **Graphene admixture particle distribution**

Fig. 1 presents the particle size distribution of the graphene admixture in aqueous dispersion used in this study, measured by dynamic light scattering. The distribution follows a unimodal, approximately log-normal profile centred around a mean hydrodynamic diameter of 816 nm, with the majority of particles falling within the 200-2000 nm range. The relatively narrow distribution indicates a well-stabilised colloidal suspension with limited coarse-particle aggregation at the upper tail. This sub-micron particle size range is of direct relevance to the intended reinforcement mechanism. Particles in this size regime are sufficiently small to permeate the interstitial pore network of the cement paste matrix and act as heterogeneous nucleation sites for C-S-H gel formation, while remaining large enough to retain the platelet morphology characteristic of few-layer graphene. The absence of a secondary coarse population suggests that the surfactant stabilisation effectively suppresses reaggregation under ambient storage conditions [22].

## Results and discussion

Fig. 2 presents the relative change in 24-hour compressive strength across the conventional additive dosage range (0.02-0.10% pure graphene by binder mass) for all three binder systems. Results are reported as percentage change relative to the GNP-free reference mix for each binder type, with error bars indicating the range between the two specimens tested. CEM III/B exhibited the most severe and consistent strength reductions of all systems tested, with reductions increasing progressively from approximately 5% at 0.02% dosage rate to around 20% at the highest dosage of 0.10%. The error bars for CEM III/B are notably narrow throughout, indicating a consistent response between replicate specimens and while this is encouraging, the limited replication means the trend cannot be statistically verified and should be interpreted with appropriate caution.

CEM II/B-M showed modest and relatively stable reductions across the dosage range, generally remaining within 1% to 6%, with no clear dose-dependent trend. This comparatively minor response at conventional dosages is consistent with its more favourable behaviour in the microdosing series. CEM I showed small reductions at lower dosages but notably crossed into positive territory at 0.10%, reaching approximately 3%, suggesting a slight densification effect at higher dosages in the absence of slag. The wider error bars for CEM I at several dosages indicate greater variability between the two specimens and warrant cautious interpretation. Across all systems, the severity of strength reduction broadly correlates with slag content, with CEM III/B > CEM II/B-M > CEM I, consistent with a binder-

chemistry-dependent interaction between the surfactant carrier and the cementitious matrix. Similar response was observed also for 7 day and 28 day results.

The slag-content-dependent severity of strength reduction is consistent with the known sensitivity of GGBS-containing systems to polycarboxylate ether (PCE) admixtures. Palacios et al. [23] demonstrated that PCE superplasticisers can substantially retard slag activation in blended cements, attributing this to surfactant adsorption on slag particle surfaces that reduces the rate of glass network dissolution, a reaction particularly sensitive to the availability of alkali ions released during early Portland clinker hydration. In high-slag systems, where clinker content and therefore early alkalinity is limited, any surfactant-driven suppression of this activation window is expected to produce a disproportionately large early-age strength penalty, consistent with the CEM III/B results observed here. In contrast, the CEM I system lacks slag and would not be subject to this mechanism, the small positive density and strength response recorded at the highest conventional dosage may instead reflect a minor nano-filler densification effect from the GNP particles themselves. Wang et al. [18] reported microstructural densification in GNP–Portland cement composites, and Du et al. [16] observed reduced porosity and improved pore structure in CEM I systems with GNP additions at comparable dosages of 0.02-0.06% by binder mass. It should be emphasised that these mechanistic inferences are drawn indirectly from macroscopic strength and density trends, direct confirmation would require complementary measurements such as hydration calorimetry, air-content testing, or electron microscopy, which were outside the scope of this study.

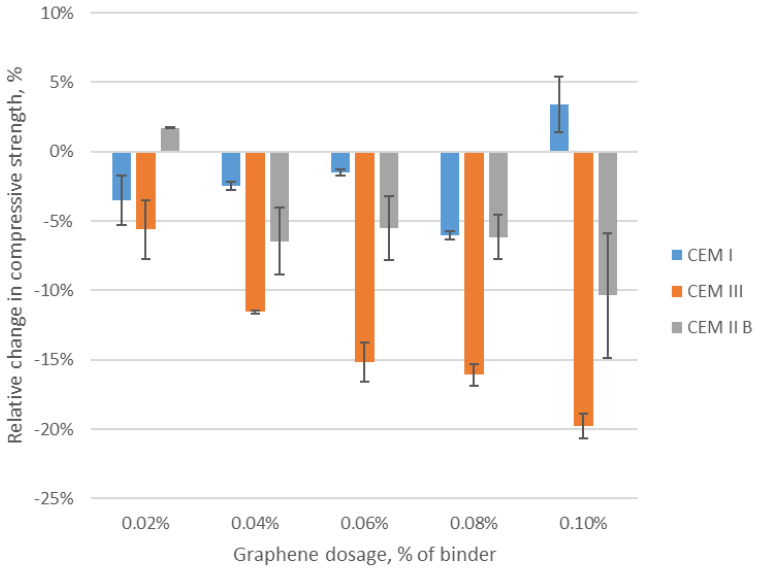


Fig. 2. **Relative compressive strength change for conventional graphene dosage series at 24 hours**

Hardened specimen density, determined according to EN 12390-7 water immersion, is retained as a diagnostic of the binder–surfactant interaction mechanism (Fig. 3). Both slag-containing systems, CEM III/B and CEM II/B-M, exhibit a net downward density trend with increasing GNP admixture dosage, consistent with progressive surfactant-induced air entrainment. The density reduction is modest in absolute terms (less than 1.25% across the full dosage range) but systematic and directionally consistent. Pure CEM I shows the opposite trend, with density increasing slightly with dosage after an initial sharp decline. This three-way divergence suggests that the cement–surfactant interaction is binder-specific. Given the limited number of data points per system ($n$ = 5), the trend lines in Fig. 3 are presented as indicative only, no curve-fitting statistics are reported.

The surfactant-induced air entrainment interpretation is supported by the known surface-active behaviour of PCE polymers. The proposed mechanism is consistent with well-established surfactant behaviour: PCE-type dispersants reduce surface tension in aqueous systems and can stabilise air voids when not fully adsorbed onto solid surfaces [23]. In slag-rich blends, the reduced Portland clinker surface area leaves a greater proportion of surfactant molecules free in solution, increasing the likelihood

of foam stabilisation. The observation that density reductions are systematically greater for CEM III/B than for CEM II/B-M, and absent or reversed for CEM I, is qualitatively consistent with this mechanism, and aligns with the PCE-slag interaction reported by Palacios et al. [23]. The modest absolute magnitude of density change (under 1.25%) nonetheless limits the strength of this inference: while systematic, such small density shifts are at the margin of what can be reliably interpreted from water immersion measurements alone. Air-content measurements would be required to confirm the presence and extent of entrained porosity and are recommended for future studies extending this work.

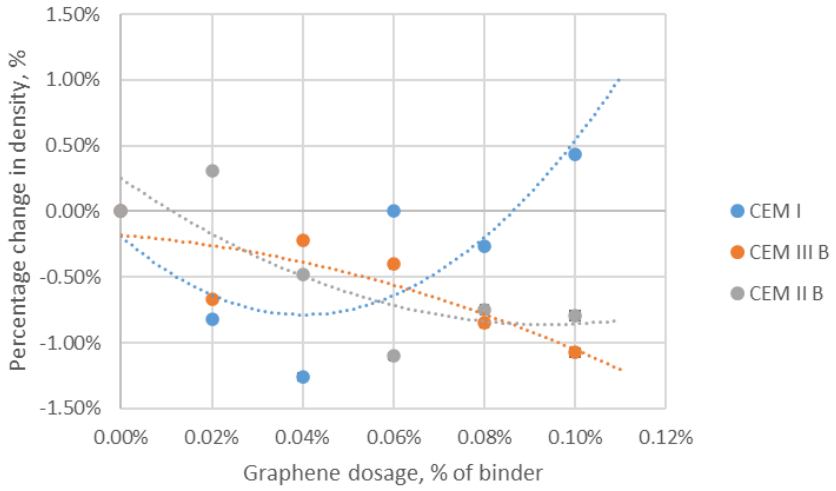


Fig. 3. **Percentage change in hardened specimen density vs GNP admixture dosage – conventional series (CEM I, CEM III/B, CEM II/B-M)**

Fig. 4 presents the relative change in compressive strength at 24 hours, 7 days, and 28 days for CEM II/B-M at w/c 0.50 across the microdosing range (0.0002-0.0014% pure graphene by binder mass or 0.02-0.09% graphene additive dosage) with reference compressive strength being 23.4 MPa for 24 hours, 51.2 MPa for 7 days and 62.5 MPa for 28 days. At the lowest dosages (0.0002-0.0005%), positive gains are observed at 24 hours, reaching around 5% (1.3 MPa), indicating that at these ultra-low concentrations, the heterogeneous nucleation benefit outweighs any surfactant retardation for this system.

Heterogeneous nucleation of C-S-H on high-surface-area substrates is well established for nano-silica and for graphene oxide in Portland cement systems [10-13], and has been proposed for few-layer graphene nanoplatelets by Wang et al. [18] and Du et al. [16] on the basis of microstructural observations in CEM I systems. The present results do not allow direct verification of this mechanism, as no hydration calorimetry or microstructural data were collected, however, the observation of strength gains persisting to 28 days argues against the effect being purely a kinetic artefact. A transient nucleation acceleration without additional C-S-H formation would be expected to produce early gains that diminish as long-term hydration equalises the degree of reaction across treated and untreated mixes. The sustained 28-day response is instead consistent with a modest increase in C-S-H nucleation density, as described by Pan et al. [10] for graphene oxide additions to Portland cement paste at conventionally reported dosages of 0.05-0.10% by binder mass – roughly two orders of magnitude higher than the pure graphene content applied here. Notably, the improvement magnitude observed in the present work (up to 5% at 24 hours and 4% at 28 days for CEM II/B-M) is modest relative to the 15-40% gains reported for GO at those higher dosages, which is consistent with the expectation that nucleation seeding efficacy scales with the number density of active sites.

The 7 day results remain unchanged for all of the samples except for the graphene dosage 0.0005%. Notably, strength gains remain positive at 28 days across nearly the full dosage range tested, with 28-day gains of 1 to 4% or (0.7-2.3 MPa) sustained even at dosages where 24-hour results showed a decline. Given the limited replication, these differences cannot be statistically confirmed, however, the directional consistency across multiple dosages and ages suggests that the GNP dispersion effect in CEM II/B-M is not confined to early age and may persist through medium-term strength development.

The decline in 24-hour compressive strength increase with increasing dosage, possibly reflects the competing surfactant retardation effect becoming more pronounced as the graphene admixture dosage rises, while the sustained 28-day response indicates that additional C-S-H formation around GNP surfaces continues to contribute as the matrix cures.

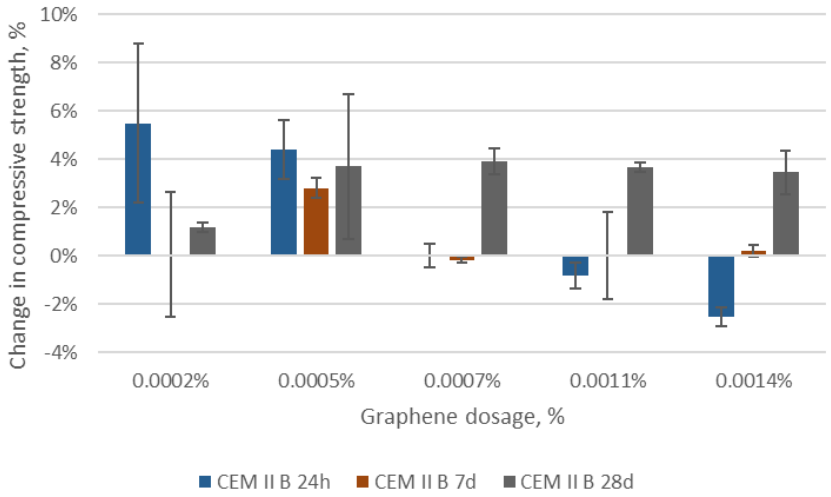


Fig. 4. **Relative change in compressive strength at 24 h, 7 d, and 28 d vs pure graphene dosage for CEM II/B-M, microdosing series**

Fig. 5 shows results for CEM III/B 32.5N in the microdosing sample set. In contrast to CEM II/B-M, CEM III/B shows strength reductions at all three tested ages and across the full dosage range, with reference compressive strength being 2.5 MPa for 24 hours, 29.8 MPa for 7 days and 51.9 MPa for 28 days. At 24 hours, reductions reach approximately 4 to 11%, with the most severe values at mid-range dosages. At 7 days, the reductions are more severe, reaching 15% at the worst dosage, before partially recovering at 28 days. This partial convergence toward neutral behaviour at 28 days relative to the larger 7 day deficits is consistent with temporary rather than permanent retardation. Delayed slag hydration recovers progressively over time, however, not reaching the reference strength. The severity of the 7 day response, exceeding the 24 hour loss in relative compressive strength for most dosages, suggests that the surfactant continues to compromise slag activation during the critical secondary hydration phase, a window in which CEM III/B is particularly sensitive [6; 23].

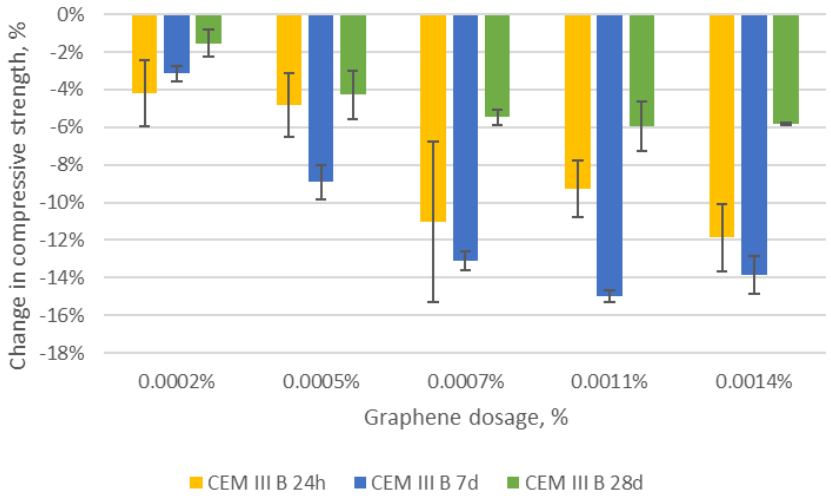


Fig. 5. **Relative change in compressive strength at 24 h, 7 d, and 28 d vs pure graphene dosage for CEM III/B 32.5N, microdosing series**

This finding is broadly consistent with the only prior studies known to the authors that examine carbon-based nanomaterials in GGBS-containing systems. Bhojaraju et al. [20; 21] investigated both

graphene and graphene oxide additions to GGBS-blended pastes and reported that the hydration-modifying effect was strongly influenced by binder chemistry, with slag systems responding differently to Portland cement controls under otherwise identical dosing conditions. While those studies focused on hydration calorimetry and fresh/hardened properties rather than early-age strength directly, the observation that GGBS systems do not uniformly benefit from graphene-type additions aligns with the negative strength responses recorded here for CEM III/B. Importantly, the pure graphene contents used in the current microdosing series (0.0002-0.0014% by binder mass) are substantially below the 0.01-0.10% range examined in those studies, indicating that the sensitivity of high-slag systems to surfactant retardation persists even at trace graphene concentrations where the nucleation contribution is expected to be minimal.

Fig. 6 presents the results for the hybrid CEM III/B + CEM I 52.5N blend, with reference compressive strength being 6.9 MPa for 24 hours, 42.0 MPa for 7 days and 70.4 MPa for 28 days. Contrary to what a simple dilution effect might predict, this system performs worse than pure CEM III/B at several dosages, with 7 day reductions reaching approximately 20 compared to 15% for pure CEM III/B. At 24 hours, reductions are in the range of around 2 to 5%, similar to CEM III/B, before a significant reduction at 7 days, where the hybrid mix shows the most severe reductions of any system tested. Partial recovery is observed at 28 days (by approximately 3 to 6%) for lower dosages, the 7 day compressive strength reduction is not recovered at higher dosages. A possible explanation is that the CEM I component accelerates early hydration sufficiently to consume the available alkalinity faster, leaving less to sustain slag activation through the critical secondary hydration window, effectively amplifying rather than buffering the surfactant retardation effect. The absence of a positive response window in the hybrid blend, even at the lowest dosage where CEM II/B-M showed gains, reinforces that the beneficial behaviour of CEM II/B-M is specific to its Portland-limestone composite chemistry rather than simply a consequence of higher clinker content.

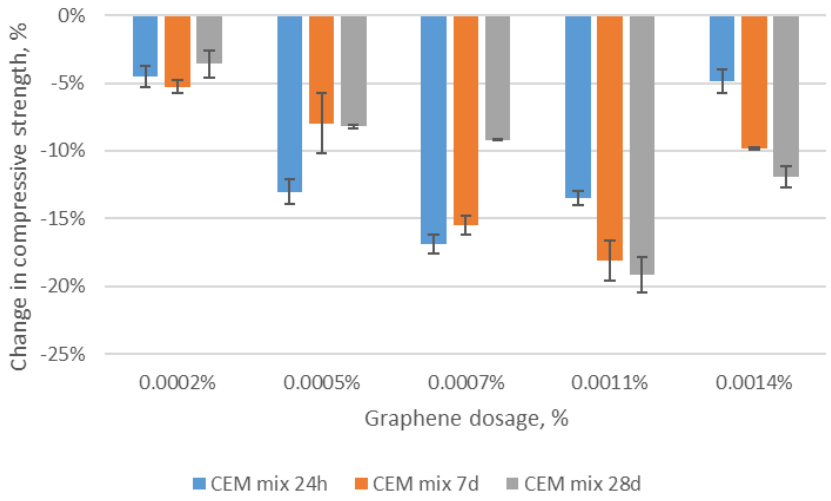


Fig. 6. **Relative change in compressive strength at 24 h, 7 d, and 28 d vs pure graphene dosage for CEM III/B + CEM I hybrid blend, microdosing series**

Flexural strength results for the microdosing series are presented in Fig. 7. Since single specimens were tested at each condition, the results are reported as individual values without error quantification and should be interpreted as indicative. Reference flexural strengths were approximately 5.4 MPa, 5.9 MPa, and 6.5 MPa for CEM III/B, CEM II/B-M, and the hybrid blend, respectively. CEM III/B showed a broadly declining trend with increasing GNP dosage, with a marginal initial rise at 0.0002% before falling to approximately 4.3 MPa at the highest dosage tested, a reduction of around 21% relative to the reference. CEM II/B-M exhibited a more complex response: flexural strength declined between 0.0002% and 0.0007%, falling to approximately 5.0 MPa, before recovering notably at 0.0011% and 0.0014%, where values of approximately 6.6 MPa were recorded, representing a gain of around 12% over the reference. The hybrid CEM III/B + CEM I blend showed consistent reductions across the intermediate dosage range, reaching a minimum of approximately 4.1 MPa at 0.0007%, before partially

recovering at higher dosages and slightly exceeding the reference value at 0.0014% (~6.8 MPa). Given that only single specimens were tested, this recovery pattern should be interpreted cautiously.

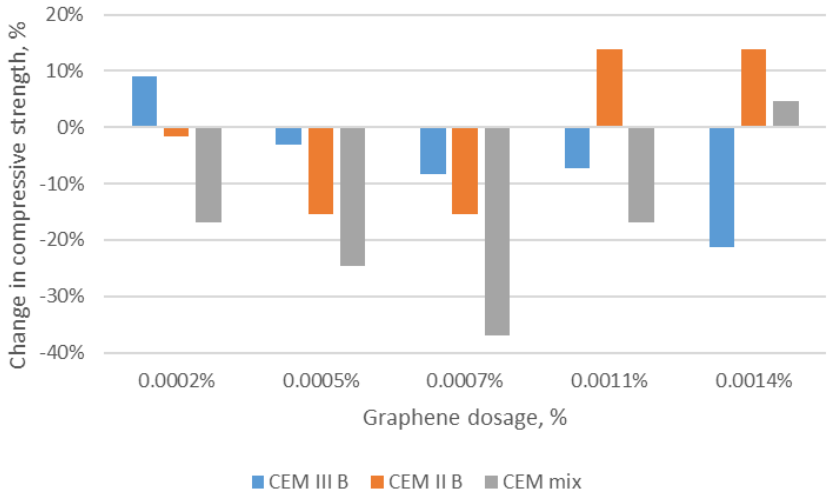


Fig. 7. **Tested flexural strength at 28 days for microdosing series of tests**

Together, the microdosing results with the tested samples listed in Table 1 for all three systems present an overall picture aligned with the conventional series findings. Strength increase or decrease, depending on the GNP dispersion in cement mortar mix, appears to be governed primarily by binder chemistry rather than graphene concentration alone, a pattern that is consistent across systems and ages despite the limited replication. CEM II/B-M, with its intermediate slag content, Portland-limestone composite chemistry, and higher early reactivity relative to CEM III/B, is the only system in which potentially the heterogeneous nucleation benefit outweighs the competing surfactant retardation effect.

## Conclusions

This study investigated the influence of a commercially available surfactant-stabilised few-layer graphene (FLG) dispersion on 24 hour, 7 day, and 28 day compressive strength development of cementitious binder systems across a conventional additive dosage range and an extended microdosing range for which, pure graphene contents fall at 0.0002-0.0014% by binder mass, one to two orders of magnitude below the minimum dosages reported in the published literature for FLG. The following conclusions can be drawn:

1. The response to GNP dispersion addition is strongly binder-dependent. In the microdosing series, only CEM II/B-M indicative positive strength trends of around 5% (1.3 MPa at 24 hours and 2.3 MPa at 28 days); CEM III/B and the hybrid blend showed reductions at all ages, with the hybrid performing worse than pure CEM III/B. These trends are based on n = 2 specimens per condition and should be interpreted as preliminary.
2. Hardened sample density provides independent evidence for binder-specific surfactant behaviour. Slag-containing systems indicated systematic density reductions up to 1.25% consistent with surfactant-induced air entrainment, while CEM I appeared to slightly densify, consistent with binder-chemistry-driven mechanism.
3. A beneficial dosage window was identified among the systems tested exclusively for CEM II/B-M, where positive compressive strength gains of up to 5% at 24 hours are sustained through 28 days, suggesting that the nucleation benefit is a durable improvement in strength development rather than a transient kinetic effect. This interpretation requires confirmation with larger sample sizes.
4. The results are based on two specimens per condition for compressive strength and single specimens for flexural strength, without formal replication sufficient for significance testing. All findings should therefore be regarded as screening-level trends requiring confirmation in a replicated experimental programme before any conclusions are drawn with statistical confidence. From a practical standpoint, these indicative results suggest that commercially available PCE-stabilised GNP dispersions are not universally suitable as early-strength accelerators in low-carbon precast

applications, and that their use should be prioritised for CEM II/B-M type binders, however, this recommendation is subject to confirmation through replicated testing.

5. Future work should prioritise microstructural analysis (SEM, MIP) to verify the proposed air entrainment and nucleation mechanisms, density measurements in the microdosing series, and investigation of surfactant-free or cement-type-tailored dispersion chemistries compatible with high-slag systems.

## Author contributions

E. Ozolins: conceptualization, experimental design, data analysis, writing. A. Macanovskis: experimental work, data collection, review, experimental supervision. N. Sinica: experimental work, data collection, review. M. Tupesis: experimental work, data collection, review.

## Acknowledgements

In accordance with the contract No. 1.2.1.2.i.2/1/24/A/CFLA/004 between "VMKC" Ltd. and the Central Finance and Contracting Agency, concluded on 26th of September 2024, the study is conducted by "Dzelzsbetons MB" Ltd. with support from the European Regional Development Fund (ERDF) within the framework of the project "Competence centre of smart materials and technologies".



## References

[1] Andrew R.M. Global $CO_2$ emissions from cement production, 1928–2018. Earth System Science Data, vol. 11, 2019, pp. 1675-1710.

[2] Scrivener K.L., John V.M., Gartner E.M. Eco-efficient cements: Potential economically viable solutions for a low-$CO_2$ cement-based materials industry. Cement and Concrete Research, vol. 114, 2018, pp. 2-26.

[3] Miller S.A., Horvath A., Monteiro P.J.M. Readily implementable techniques can cut annual $CO_2$ emissions from the production of concrete by over 20%. Environmental Research Letters, vol. 11, 2016, 074029.

[4] Juenger M.C.G., Siddique R. Recent advances in understanding the role of supplementary cementitious materials in concrete. Cement and Concrete Research, vol. 78, 2015, pp. 71-80.

[5] Lothenbach B., Scrivener K., Hooton R.D. Supplementary cementitious materials. Cement and Concrete Research, vol. 41, 2011, pp. 1244-1256.

[6] Ballim Y., Graham P.C. The effects of supplementary cementing materials in modifying the heat of hydration of concrete. Materials and Structures, vol. 42, 2009, pp. 803-811.

[7] Oner A., Akyuz S. An experimental study on optimum usage of GGBS for the compressive strength of concrete. Cement and Concrete Composites, vol. 29, 2007, pp. 505-514.

[8] Novoselov K.S., Geim A.K., Morozov, S.V., et al. Electric field effect in atomically thin carbon films. Science, vol. 306, 2004, pp. 666-669.

[9] Zhu Y., Murali S., Cai W., et al. Graphene and graphene oxide: synthesis, properties, and applications. Advanced Materials, vol. 22, 2010, pp. 3906-3924.

[10] Pan Z., He L., Qiu L., et al. Mechanical properties and microstructure of a graphene oxide-cement composite. Cement and Concrete Composites, vol. 58, 2015, pp. 140-147.

[11] Mohammed A., Sanjayan J.G., Duan W.H., Nazari A. Incorporating graphene oxide in cement composites: A study of transport properties. Construction and Building Materials, vol. 84, 2015, pp. 341-347.

[12] Lv S., Ma Y., Qiu C., et al. Effect of graphene oxide nanosheets on microstructure and mechanical properties of cement composites. Construction and Building Materials, vol. 49, 2013, pp. 121-127.

[13] Chuah S., Pan Z., Sanjayan J.G., et al. Nano reinforced cement and concrete composites and new perspective from graphene oxide. Construction and Building Materials, vol. 73, 2014, pp. 113-124.

[14] Sharma S., Kothiyal N.C. Influence of graphene oxide as dispersed phase in cement mortar matrix in defining the crystal patterns of cement hydrates and its effect on mechanical, microstructural and crystallization properties. RSC Advances, vol. 5, 2015, pp. 52642-52657.
[15] Lu Z., Hou D., Meng L., et al. Mechanism of cement paste reinforced by graphene oxide/carbon nanotubes composites with enhanced mechanical properties. RSC Advances, vol. 5, 2015, pp. 100598-100605.
[16] Du H., Gao H.J., Pang S.D. Improvement in concrete resistance against water and chloride ingress by adding graphene nanoplatelet. Cement and Concrete Research, vol. 83, 2016, pp. 114-123.
[17] Parveen S., Rana S., Fangueiro R. A review on nanomaterial dispersion, microstructure, and mechanical properties of carbon nanotube and nanofiber reinforced cementitious composites. Journal of Nanomaterials, vol. 2013, 2013, 710175.
[18] Wang B., Jiang R., Wu Z. Investigation of the mechanical properties and microstructure of graphene nanoplatelet-cement composite. Nanomaterials, vol. 6, 2016, 200.
[19] Zhao L., Guo X., Ge C., et al. Investigation of the effectiveness of PC@GO on the reinforcement for cement composites. Construction and Building Materials, vol. 113, 2016, pp. 470-478.
[20] Bhojaraju C., Di Mare M., Ouellet-Plamondon, C.M. The impact of carbon-based nanomaterial additions on the hydration reactions and kinetics of GGBS-modified cements. Construction and Building Materials, vol. 303, 2021, 124366.
[21] Bhojaraju C., Mousavi S.S., Brial V., Di Mare M., Ouellet-Plamondon C.M. Fresh and hardened properties of GGBS-contained cementitious composites using graphene and graphene oxide. Construction and Building Materials, vol. 300, 2021, 123902.
[22] Lotya M., Hernandez Y., King P.J., et al. Liquid phase production of graphene by exfoliation of graphite in surfactant/water solutions. Journal of the American Chemical Society, vol. 131, 2009, pp. 3611-3620.
[23] Palacios M., Puertas F., Bowen P., Houst Y.F. Effect of PCs superplasticizers on the rheological properties and hydration process of slag-blended cement pastes. Journal of Materials Science, vol. 44, 2009, pp. 2714-2723.